HHS Public Access

Author manuscript

Vision Res. Author manuscript; available in PMC 2022 November 01.

Published in final edited form as:

Vision Res. 2021 November ; 188: 162–173. doi:10.1016/j.visres.2021.07.008.

Dependence of visual and cognitive outcomes on animal holder configuration in a rodent model of blast overpressure exposure

Rachael S. Allen[a,b], **Cara T. Motz**[a,b], **Anayesha Singh**[a], **Andrew Feola**[a,b], **Lauren Hutson**[a], **Amber Douglass**[a], **Sriganesh Ramachandra Rao**[e], **Lara A. Skelton**[d], **Lidia Cardelle**[a], **Katie L. Bales**[a,c], **Kyle Chesler**[a,b], **Kaavya Gudapati**[a], **C. Ross Ethier**[b], **Matthew M. Harper**[f,g], **Steven J. Fliesler**[d,e], **Machelle T. Pardue**[a,b]

[a]Center for Visual and Neurocognitive Rehabilitation, Atlanta VA Healthcare System, Decatur, GA

[b]Department of Biomedical Engineering, Georgia Institute of Technology, Atlanta, GA

[c]Department of Ophthalmology, Emory University School of Medicine, Atlanta, GA

[d]Research Service, VA Western NY Healthcare System, Buffalo, New York

[e]Ophthalmology, Biochemistry, and Neuroscience Program, SUNY-University at Buffalo, Buffalo, New York

[f]Iowa City VA Health Care System Center for the Prevention and Treatment of Visual Loss, Iowa City, Iowa

[g]Department of Ophthalmology and Visual Sciences, University of Iowa, Iowa City, Iowa

Abstract

Blast-induced traumatic brain injury is the signature injury of modern military conflicts. To more fully understand the effects of blast exposure, we placed rats in different holder configurations, exposed them to blast overpressure, and assessed the degree of eye and brain injury.

Anesthetized Long-Evans rats received blast exposures directed at the head (63kPa, 195 dB-SPL) in either an “open holder” (head and neck exposed; n=7), or an “enclosed holder” (window for blast exposure to eye; n=15) and were compared to non-blast exposed (control) rats (n=22).

Corresponding Author: Machelle T. Pardue, Ph.D., Atlanta VA Center for Visual and Neurocognitive Rehabilitation, Research Service (151 Oph), 1670 Clairmont Rd., Decatur, GA 30033, Telephone: (404)321-6111 X207342, Fax: (404)728-4847, machelle.pardue@bme.gatech.edu.

Credit Author Statement

Rachael S Allen: Investigation, Formal analysis, Writing-Original Draft, Writing-Review & Editing, Visualization; **Cara T Motz**: Investigation, Formal analysis, Data Curation; **Anayesha Singh**: Investigation, Formal analysis; **Andrew Feola**: Investigation, Formal analysis, Data Curation, Writing-Review & Editing; **Lauren Hutson**, Formal analysis, Writing-Original Draft, Writing-Review & Editing, Visualization; **Amber Douglass**: Investigation, Formal analysis, Writing-Review & Editing; **Sriganesh Ramachandra Rao**: Investigation, Writing-Review & Editing, **Lara A Skelton**: Investigation, Formal analysis, Writing-Review & Editing, Visualization; **Lidia Cardelle**: Investigation, Formal analysis, Writing-Review & Editing; **Katie L. Bales**: Investigation, Formal analysis, Writing-Review & Editing; **Kyle Chesler**: Investigation, Formal analysis, Writing-Review & Editing; **Kaavya Gudapati**: Investigation, Formal analysis, Writing-Review & Editing, **C. Ross Ethier**: Formal analysis, Writing-Review & Editing; **Matthew M Harper**: Investigation, Formal analysis, Writing-Review & Editing, **Steven J Fliesler**: Conceptualization, Investigation, Writing-Review & Editing, Project administration, Funding acquisition; **Machelle T Pardue**: Conceptualization, Investigation, Writing-Review & Editing, Supervision, Project administration, Funding acquisition

Outcomes included optomotor response (OMR), electroretinography (ERG), and spectral domain optical coherence tomography (SD-OCT) at 2, 4, and 6 months post-blast, and cognitive function (Y-maze) at 3 months.

Spatial frequency and contrast sensitivity were reduced in ipsilateral blast-exposed eyes in both holders ($p<0.01$), while contralateral eyes showed greater deficits with the enclosed holder ($p<0.05$). Thinner retinas ($p<0.001$) and reduced ERG a- and b- wave amplitudes ($p<0.05$) were observed for both ipsilateral and contralateral eyes with the enclosed, but not the open, holder. Rats in the open holder showed cognitive deficits compared to rats in the enclosed holder ($p<0.05$).

Overall, the animal holder configuration used in blast exposure studies can significantly affect outcomes. Enclosed holders may cause secondary damage to the contralateral eye by concussive injury or blast wave reflection off the holder wall. Open holders may damage the brain via rapid head movement (contrecoup injury). These results highlight additional factors to be considered when evaluating patients with blast exposure or developing models of blast injury.

Keywords

blast; traumatic brain injury; TBI; retina; eye

1. INTRODUCTION

Blast-mediated traumatic brain injury has become the signature injury of current military conflicts[1, 2], accounting for an estimated 60% of casualties in military settings[3]. Between 2000 and 2019, more than 410,000 service members suffered at least one traumatic brain injury (TBI), many of which resulted from blast exposure[4]. Of concern to ophthalmologists are ocular injuries arising from exposure to blast, especially since such injuries have significant and lifelong impacts. Over five million Americans are estimated to have experienced visual impairment following blast exposure[5] that resulted in partial or complete damage to their visual system[6-9]. While penetrating eye injuries are readily diagnosed and managed within the military's casualty care system[10], non-penetrating (closed-globe) ocular injuries may not be readily apparent[11]. In one prospective case series of 46 blast-exposed veterans, 43% had non-penetrating ocular injury[12]. Visual deficits post-blast exposure include reading difficulties, reduced contrast sensitivity, accommodation issues, visual field changes, diplopia, and photosensitivity[13-17]. Importantly, visual symptoms may not present until weeks, months, or even years after blast exposure[12, 13]. Thus, estimates of visual dysfunction resulting from blast exposure are likely underestimated[18].

Blast injury is categorized as primary, secondary, or tertiary according to the anatomical and physiological changes from the blast wave impacting the body's surface[19]. Primary injury results directly from the blast wave and the consequent changes in air pressure, with rapid tissue deformation and destruction resulting from the intense over-pressurization. Secondary injury results from flying debris and bomb fragments. Tertiary injury results from individuals being thrown by the blast wind[20]. Following blast exposure, the rotational and translational forces from the blast wave result in diffuse axonal injury and

exacerbate pathology in the brain[21-23]. The main mechanisms attributed to blast exposure are acceleration-deceleration, direct cranial transmission of the blast wave, and thoracic transmission[22-24]. Head acceleration is a major contributor to injury; in addition to damage to neurons and glia (particularly the axons that make up the white matter) caused by shear force and stretching[25], the direct transmission of the blast wave through the skull can also contribute to neural damage[24].

Blast-related injuries are studied in mice and rats due to their low cost, ease of genetic manipulation, and well-mapped genomes[26]. Blast experiments conducted using rats and mice have included free-field explosions[27-29], shock tubes[30, 31], and modified devices such as a nail gun[28] and a paintball gun[32, 33]. In these blast models, peak overpressures and durations are documented in an effort to ensure that experimental design produces blast exposure conditions comparable to those experienced by military personnel[24, 34]. Though open field explosions are most accurate in representing the complex clinical situation of blast exposure in combat, the other models above allow for the isolation of specific parameters of interest because blast injury can be constrained to the entire head, specific regions of the brain, or the orbit. Furthermore, occurrence of unilateral ocular injury in humans from eye-directed blasts supports experimental modeling of unilateral ocular injury[35]. Many groups focus on retinal pathology in animal models, both to study the visual consequences of blast exposure and to evaluate damage to the CNS using the retina as an accessible proxy[7, 30, 32, 33, 36, 37]. Assessments of neural pathology in mice following blast exposure have revealed damage to axonal tracts in the brain[38], in addition to delayed onset damage in retinal ganglion cell (RGC) axonal tracts, photoreceptors, and cells within the inner nuclear layer[7, 36]. Blast exposure additionally induces traumatic head acceleration in blast neurotrauma models and links blast exposure with the development of chronic traumatic encephalopathy (CTE)-like neuropathology[34].

In addition to the blast model chosen, we hypothesized that the type of holder configuration used to immobilize test animals during blast exposure could affect the blast-associated phenotype with regard to brain and retinal pathology. In the present study, we assessed how different animal holder configurations used in a blast overpressure model affected the magnitude of both eye and brain injury by longitudinally evaluating the effect of the blast wave on the visual system and the brain over a time course of several months.

2. MATERIALS AND METHODS

2.1 Animals and experimental design

The following experiments were approved by the Atlanta Veterans Affairs and the VA Western New York Healthcare System (VAWNYHS) Institutional Animal Care and Use Committees and abided by the *ARVO Statement for the Use of Animals in Ophthalmic and Vision Research* and *National Institutes of Health Guide for the Care and Use of Laboratory Animals* (NIH Publications, 8th edition, updated 2011). Adult male Long Evans outbred rats (Blue Spruce, HsdBlu:LE; Envigo; n = 55) were utilized in this study. Rats were housed in shoe-box style cages with chow and water provided *ad libitum* on a 12:12 light:dark cycle (light onset at 6:00 AM). Blast exposure was performed at the Buffalo VA Medical Center on rats that were approximately 3.5 months of age (420-450 g). Rats were positioned in front

of the blast tube in either an “open holder” or an “enclosed holder”. The open holder group (n = 7) and enclosed holder group (n = 15) were run in separate cohorts with their own non blast-exposed controls (open group controls: n = 10, enclosed group controls: n = 12). Seven rats from the open group and two rats from the enclosed group died following blast exposure. Two rats from the enclosed group appeared to have retinal degeneration based on significant retinal thinning; therefore, they were considered outliers using the ROUT[39] (the Robust regression and OUTlier removal) method (GraphPad) and excluded from this study.

After a 1-month recovery period following blast exposure, rats were shipped to the Atlanta VA Healthcare System. Optomotor response (OMR), electroretinography (ERG), and spectral-domain optical coherence tomography (SD-OCT) recordings were acquired at 2, 4, and 6 months post-blast to investigate visual and retinal function and structure (see details in Sections 2.4-2.6). In addition, Y-maze testing was performed at 3 months post-blast to analyze cognitive function (see details in Section 2.7). The rats were euthanized at 6 months post-blast exposure and eyes and brains collected for future analysis.

2.2 Blast overpressure model

Blast exposure was performed as described previously[40]. Briefly, rats were anesthetized via intramuscular injection with a ketamine (75 mg/kg)/xylazine (15 mg/kg) mixture. Corneas were anesthetized with proparacaine hydrocholoride (0.5% ophthalmic solution, Akorn, Inc., Lake Forest, IL; 1–2 drops/eye). Then, rats were exposed to a closed-globe acoustic blast using a modified shock tube device. The blast utilized an 80-psi backpressure load of compressed nitrogen in the driver section of the shock tube to generate a sound pressure level of *ca*. 190 dB SPL (sound pressure ~63 kilopascals [kPa]). A standard pressure gauge was mounted on the shock tube body to measure backpressure load (80 psi). A pressure sensor (Model 137A23 ICP Pressure Sensor; PCB Piezotronics, Depew, NY.) was placed at the outlet (mouth) of the shock tube to measure sound pressure (db SPL). To generate the blast, a computer-controlled amount of nitrogen gas was allowed to build up inside the driver section of the shock tube behind a brass foil diaphragm held in place by O-rings. Then, a solenoid-driven arrow inside the tube was driven forward via computer to rupture the foil, release the backpressure, and cause an instantaneous acoustic shockwave. Either the left or right eye was positioned in front of the blast tube and analysis was conducted on both the ipsilateral and contralateral blast-exposed eyes. Eyes were open during blast exposure.

After blast exposure, an anesthesia reversal agent, Antisedan® (Atipamezole HCl, 1 mg/kg, Zoetis Inc., Parsippany-Troy Hills, NY), was injected intraperitoneally to speed the waking process and reduce the risk of corneal ulcers[41]. Antibiotic ointment (gentamycin sulfate, 0.3% ophthalmic ointment; Akorn, Inc.) was applied to both eyes (primarily to preserve corneal hydration during recovery), and rats were returned to their cages, where body temperature was maintained with heating pads until the rats became ambulatory. Blast overpressure-exposed rats received subcutaneous injections of buprenorphine (Buprenex, 0.05 mg/kg) prophylactically for analgesia approximately 30–40 min after Antisedan® administration (to avoid a drug interaction-induced respiratory failure) and again 24 h post-blast. Rats were monitored carefully for vital signs and any signs of pain or distress following blast exposure.

2.3 Open and Enclosed holders

During blast exposure, rats were positioned in one of two animal holding chambers (Fig. 1). For both holders, the blast exposure was directed at one side of the head, perpendicular to the body axis, with the head 2.5 inches from the end of the muzzle of the shock tube.

The open holder encased the body of the animal such that only the head was exposed. The head was supported by a roll of gauze placed under the animal's chin and was not restrained (Figure 1A, 1B). Thus, the head was able to move about freely in response to the blast, although a large standard pillow was placed against the contralateral side of the head to partially reduce the range of motion and impact to the contralateral eye. The pillow (foam, with cotton casing; *ca*. 24 in. (L) x 16 in. (W), and *ca*. 8 in. in thickness) was placed in direct contact with the contralateral side of the animal's head and runs the entire length of the animal holder in parallel (in line with the anterior-posterior line of the body), extending *ca*. 10-12 in. beyond the tip of the animals' nose. Hence, it covers the whole area of projected blast wave propagation. A solid support is placed behind the pillow, to maintain its position.

The enclosed holder had the rat's head and body encased entirely within the apparatus with the blast being delivered to the eye through a 2.5 in. x 2.5 in. window (Figure 1C). A microfiber sponge was placed between the contralateral side of the animal's head and the interior wall of the holder, providing a cushion to reduce the likelihood of direct concussive injury (*e.g.*, compression or implosion of the contralateral eye).

High speed observations of live blast exposures were used to visualize the rats' head movements in response to blast exposure using both open and enclosed holders (n = 3/group). A high-speed Phantom V2012 camera (Ametek, Wayne, NJ) was used to capture footage at 3000 frames per second during blast exposure. Head movement during blast exposure was qualitatively analyzed using high-speed videography. These experiments were performed at the Iowa City VA (the location of the camera) using a different shock tube, but the exact holders were shipped from Buffalo, NY.

2.4 Optomotor response (OMR)

A virtual OMR tracking system was used to measure the rats' visual function (OptoMotry®; Cerebral-Mechanics, Lethbridge, AB, Canada) as previously described[42-44]. Rats were placed on a circular platform in the center of a virtual reality chamber composed of four computer monitors, which present vertical sine wave gratings revolving at a speed of 12 deg/sec. A video camera monitored the animals' behavior in real time throughout the experiment. The presence or absence of reflexive movements by the rat's head were noted as it tracked the rotating gratings moving either in a clockwise or counter-clockwise direction. When rats became distracted, their attention was regained by gently tapping the instrument. OptoMotry® uses a staircase paradigm to automatically calculate spatial frequency and contrast sensitivity thresholds. To evaluate spatial frequency, contrast was held constant at 100% while spatial frequency gratings started with a frequency of 0.042 cyc/deg and adjusted over time with the presence or absence of head movements. To assess contrast sensitivity, spatial frequency was held constant at the peak of the contrast sensitivity curve at 0.064 cyc/deg (for rats), while contrast began at 100% and adjusted over time. The contrast

sensitivity reported here was calculated as a reciprocal of the Michelson contrast from the screen's luminance (max+min/max−min), as previously described[45].

2.5 Electroretinography (ERG)

Electroretinography (ERG) was used to evaluate retinal function, as described previously[46]. Prior to ERG testing, rats were dark-adapted overnight and anesthetized with a mixture consisting of ketamine (60 mg/kg) and xylazine (7.5 mg/kg). Rats older than 6 months were given a ketamine-only booster if they required additional anesthesia. The rats' corneas were anesthetized with 1% tetracaine, and their pupils were dilated with 1% tropicamide. Reference electrodes were placed in each cheek subcutaneously, while ground-needle electrodes were placed in the tail. Custom gold loop electrodes to directly measure retinal responses were placed on each corneal surface under a methylcellulose layer. ERG stimuli were presented under scotopic conditions in a Ganzfeld dome. Testing comprised five steps of full-field flashes (−3.0 to 2.1 log cd sec/m^2) with a commercial system (UTAS Big Shot, LKC Technologies, Gaithersburg, MD). Responses had a 250 msec recording length, and retinal function was permitted to recover between steps with intervals of 2 to 70 seconds with the brightest flashes having the longest interflash intervals. Responses were run through a 0.3–500 Hz bandpass filter. After the brightest dark-adapted flash, rats were light adapted at 30 cd sec/m^2 for 10 min and a flicker ERG was performed (2.0 log cd sec/m^2 at 6 Hz). Amplitudes and implicit times were measured for a-waves from baseline to trough and represent photoreceptor cell function; b-waves from trough to peak and represent bipolar cell function; flicker b-waves from trough to peak and represent a cone pathway response; and oscillatory potentials (OPs), which are characteristic wavelets on the leading edge of the b-wave, are thought to represent inner retinal function. OPs were filtered off-line using a 75–500 Hz filter (EM for Win version 9.4.0, LKC Technologies) and individual OP waves were measured for amplitudes and implicit times.

2.6 Spectral domain optical coherence tomography (SD-OCT)

An SD-OCT system (Bioptigen R4300, Leica Microsystems, Buffalo Grove, IL) was used to assess retinal structure as described previously[47]. Rats were anesthetized with a mixture consisting of ketamine (60 mg/kg) and xylazine (7.5 mg/kg) and given topical corneal anesthesia (tetracaine 1%) and pupil dilation (tropicamide 1%). The rat was then placed in a rodent alignment system and its eye was positioned in front of the SD-OCT scan head. The 3 mm radial scan was centered at the optic nerve for each eye. 1000 a-scans per b-scan were taken, with four b-scans composed of 24 frames per scan being imaged. Nasal to temporal and superior to inferior scans were analyzed.

B-scan images were evaluated manually by a trained technician via a customized MATLAB program (Mathworks, Matlab R2017a, Natick, MA) that allows markers to be placed manually at the bounds of each retinal layer. The program then calculated each layer's thickness in microns. The retinal layers included: retinal nerve fiber layer (RNFL), inner plexiform layer (IPL), inner nuclear layer (INL), outer plexiform layer (OPL), outer nuclear layer (ONL), external limiting membrane (ELM), inner segments/outer segments (IS/OS), and retinal pigment epithelium (RPE). Total retinal thickness (TRT) was defined as the difference from the inner limiting membrane to the boundary of the RPE. B-scan images

were captured at four different locations relative to the optic nerve: superior, inferior, nasal, and temporal. Additionally, two retinal distances from the optic nerve head were assessed in each of the four quadrants, with 0.5 mm representing the central retinal and 1.2 mm representing the peripheral retina (Figure 2). Retinal quadrant measurements did not show consistent and significant differences and thus were averaged to provide one value for each retina at each location. Analysis of differences between groups at each retinal location was then examined. Only data from the 0.5 mm location are presented since no differences were found at the 1.2 mm location.

2.7 Y-maze

A Y-maze was used to assess cognitive function (spatial alternation) and exploratory behavior (number of entries), as described previously[44, 48]. The maze (San Diego Instruments, San Diego, CA) is in the shape of a Y with each arm being labelled A, B, or C. Each rat was placed in arm B near the center and permitted to explore the maze for 8 min. In this time, each entry into an arm was recorded with an entry being defined as all four limbs passing into an arm. A sequence of entries was designated as an “alternation” if the rat entered into three different arms consecutively (*e.g.*, ABC, CAB). The final spatial alternation score was computed by dividing the number of alternations by the number of potential alterations that could have been completed (total entries minus two).

2.8 Immunohistochemistry

Eyes were harvested from each holder group at 6 or 8 months post blast exposure alongside age-matched, non-exposed controls. Eyes were enucleated and immersion fixed overnight at 4°C in phosphate buffered saline containing 3.7% (w/v) formaldehyde (prepared from paraformaldehyde (PFA); Electron Microscopy Sciences [EMS] Hatfield, PA) as described previously[40]. Fixed eyes were paraffin-embedded and sectioned (10 μm-thickness) at the Research Microscopy and Histology Core, Department of Pathology, Saint Louis University (St. Louis, MO), per a fee-for-service agreement. Following de-paraffinization and rehydration, antigen retrieval was performed by incubation in Envision Flex Low pH target retrieval solution (#K8005; Agilent, Santa Clara, CA) at 95°C for 20 min. For immunohistochemistry, tissue sections were blocked in tris-buffered saline plus 0.1% (v/v) TWEEN-20 (TBST) containing nonimmune goat serum at 5% (v/v), 0.5% (w/v) BSA, and 0.5% (w/v) fish skin gelatin at room temperature for 30 min followed by incubation with anti-glutamine synthetase monoclonal antibody (1:250 in TBST, clone 6, #610517; BD Biosciences, San Jose, CA), overnight at 4°C in a humidified chamber. Following three rinses in TBST, sections were incubated with secondary antibody (F(ab’)2-goat anti-rabbit IgG [H+L], conjugated with AlexaFluor®-647 (1:500 in TBST, #A21246, Thermo Fisher Scientific, Grand Island, NY), for 1 hour at room temperature. Sections were rinsed three times in TBST, followed by one rinse in TBS and nuclei counterstained with 4′,6-diamidino-2-phenylindole (DAPI, 1 μg/ml). Slides were then dipped in distilled water, and coverslips applied using Fluoro-Gel™ mounting media (#17485-40, EMS). Sections were examined with a Leica TCS SPEII DMI4000 scanning laser confocal fluorescence microscope. Images were captured using the 40X oil immersion (RI-1.518) objective under nominal laser intensity (10–22% of maximum intensity), arbitrary gain (750) and offset (−0.5) values, to optimize the signal-to-noise ratio.

2.9 TUNEL labeling

For TUNEL labeling, tissue sections from both holder groups (and age-matched controls) were deparaffinized and antigen retrieved as described above. Sections from the holder groups were compared to a positive control similarly processed: paraffin-embedded eye sections from AY9944-treated rats [a pharmacological model of Smith-Lemli Opitz Syndrome (SLOS), characterized by severe retinal degeneration] at 80 days of age[49]. Apoptotic cells were detected using dUTP-biotin nick-end labelling (TUNEL Andy Fluor™ 647 Apoptosis Detection Kit, #A052, ABP Biosciences, Beltsville, MD), following the manufacturer's instructions with some modifications. Briefly, sections were incubated with terminal deoxynucleotidyl transferase and biotin-11-dUTP for 90 minutes at room temperature. Sections were then washed 3 times in PBS followed by incubation with Streptavidin conjugated to AlexaFluor®-488 (1:500 in PBS, #S32354 Thermo Fisher Scientific) at 4°C overnight. Sections were washed three times in PBS, counterstained with DAPI and mounted as described above. Sections were examined with a Leica TCS SPEII DMI4000 scanning laser confocal fluorescence microscope. Images were captured using the 40X oil immersion (RI-1.518) objective under nominal laser intensity (10–22% of maximum intensity), arbitrary gain (700) and offset (−0.5) values, to optimize the signal-to-noise ratio.

2.10 Statistical analysis

Results are presented as mean ± standard error of the mean (SEM). The two control groups were found to not differ from each other on OMR, SD-OCT, and Y-maze outcomes, and were thus combined (n = 22). For ERG, the two control groups were found to be distinct, so data is presented as both separated by cohort and as normalized data (more information in Results, Section 3.2). Prism (GraphPad) software evaluates whether data are normally distributed and runs a mixed-effects ANOVA model (REML; REstricted Maximum Likelihood) instead of a two-way repeated measures (RM) ANOVA if a normal distribution is not found. As a result, a mixed-effects ANOVA model (REML) was used to analyze ERG and OP data. Two-way RM ANOVAs followed by Holms-Sidak post hoc tests for individual comparisons were used to evaluate OMR and SD-OCT data. A one-way ANOVA followed by Holms-Sidak tests for individual comparisons was used to evaluate Y-maze data. Statistical analysis was performed with SigmaPlot 13.0 (Systat Software, Inc., San Jose, CA) or Prism 8.0 (Graphpad Software, Inc, San Diego, CA).

3. RESULTS

3.1 Visual function deficits differed in the contralateral blast-exposed eyes depending on holder configuration

Ipsilateral eyes of rats exposed to blast in either the open or enclosed holder showed significant deficits in spatial frequency (correlates with visual acuity) and contrast sensitivity that were similar in magnitude and progression. Meanwhile, OMR deficits in contralateral eyes were dependent on the type of holder employed.

For rats immobilized in the open holder, spatial frequency deficits were only observed in the ipsilateral eyes exposed to blast compared with non-blast (two-way RM ANOVA interaction effect, group x timepoint, $F[8,107] = 3.616$, $p < 0.001$), with the contralateral

eye showing similar values to non-blast-exposed controls (Fig. 3A). Conversely, for rats immobilized in the enclosed holder, similar spatial frequency deficits were observed in both the blast-exposed ipsilateral ($p < 0.001$) and contralateral eyes ($p < 0.001$, Fig. 3A) compared to non-blast controls.

Contrast sensitivity results mirrored spatial frequency results, with the contralateral eyes of rats in the enclosed holder showing greater deficits than the contralateral eyes of rats in the open holder. For open holder rats, contrast sensitivity deficits were observed in the ipsilateral eye exposed to blast (two-way RM ANOVA interaction effect, group x timepoint, $F[8,107] = 3.434$, $p < 0.001$), with a trend for a decline observed in the contralateral eye (Fig. 3B). For rats in the enclosed holder, similar contrast sensitivity deficits were observed in both the ipsilateral eye exposed to blast ($p < 0.001$) and in the contralateral eyes ($p < 0.01$, Fig. 3B) compared to non-blast controls.

3.2 ERG a- and b-wave amplitudes were reduced only with the enclosed holder

Figure 4 shows representative ERG waveforms from control and blast-exposed rats, using either the open holder or enclosed holder, at 6 months post-blast. For the open holder group, no significant differences were observed for a- and b- wave amplitudes when comparing ipsilateral and contralateral blast-exposed eyes to eyes from the control group (Fig. 5A, 5D). However, for the enclosed holder, both ipsilateral and contralateral blast-exposed eyes showed a significantly lower amplitude compared with eyes from control group for a-wave (Mixed-effects model, main effect of group, $F[2,41] = 3.546$, $p < 0.05$, Fig. 5B), with a trend for reduced b- wave amplitudes (Mixed-effects model, main effect of group, $F[2,39] = 2.515$, $p = 0.09$, Fig. 5E). ERG a- and b- wave amplitude values obtained from rats using both open and enclosed holders were normalized to their respective controls because differences in amplitude (14.6% for a- wave, 14.2% for b- wave) were observed between the two control cohorts, which were tested months apart, a phenomenon which could be due to litter effects, differences in gold loop electrodes, or seasonal differences in the environment that affected the quality of the recordings. By normalizing to controls, a- and b- wave amplitudes could be compared directly between rats exposed to blast in the open and enclosed holders. When normalized, rats in the enclosed holder group displayed significantly lower amplitude measures for both a- waves (Mixed-effects model, main effect of group, $F[3,40] = 3.116$, $p < 0.05$, Fig. 5C) and b- waves (Mixed-effects model, main effect of group, $F[3,38] = 4.326$, $p < 0.05$, Fig. 5F) compared to controls.

Significant differences were also observed in OP1 amplitudes. Supplemental Figure 1 shows representative OP waveforms at 6 months post-blast exposure. For the open holder group, ipsilateral blast-exposed eyes were similar to eyes from the control group but showed higher amplitudes than contralateral blast-exposed eyes (Mixed-effects model, main effect of group, $F[1.356,40.67] = 9.171$, $p < 0.01$, Supplemental Figure 2A). For the enclosed holder group, contralateral blast-exposed eyes showed significantly lower OP1 amplitudes compared with ipsilateral blast-exposed eyes and eyes from the control group (Mixed-effects model, interaction effect, group x flash intensity, $F[8, 118] = 5.145$, $p < 0.001$, Supplemental Figure 2B). When normalized, these effects persisted (Mixed-effects model, interaction

effect, group x flash intensity, F[12, 138] = 4.292, $p < 0.001$, Supplemental Figure 2C). Differences in amplitude were not observed in OP2-4.

Implicit time differences were not observed for any ERG component in rats exposed to blast using either holder (data not shown). ERGs taken at 2 and 4 months post-Blast were similar to the 6-month ERGs presented here, with ipsilateral and contralateral blast-exposed eyes for the enclosed holder group showing reduced amplitudes compared with controls (data not shown).

3.3 Thinner retinas for ipsilateral and contralateral eyes were observed only with the enclosed holder

Figure 6 shows representative SD-OCT images at 6 months post-blast exposure. Total and individual layer retinal thicknesses were quantified at 2, 4, and 6 months post-blast (Fig. 7). No significant differences in total retinal thickness were observed with the open holder, though there was a trend towards reduced thickness in contralateral blast-exposed eyes compared with eyes from control rats (Fig. 7A). Decreased total retinal thickness (4%) was observed in ipsilateral and contralateral eyes from blast-exposed rats compared to eyes from control rats using the enclosed holder, beginning at 2 months post-blast and persisting to 6 months (two-way RM ANOVA interaction effect, group x timepoint, F[2,70] = 11.864, $p < 0.001$; Fig. 7B). The external limiting membrane (ELM) was consistently thinner (18%) in both ipsilateral and contralateral eyes from blast-exposed rats compared to eyes from control rats when using the enclosed holder (two-way RM ANOVA interaction effect, group x timepoint, F[2,68] = 7.08, $p < 0.01$; Fig. 7D). However, significant differences were not observed in ELM thickness when using the open holder (Fig. 7C). Significant differences were not found for other retinal layers when comparing ipsilateral *vs.* contralateral blast-exposed eyes or comparing either to non-blast-exposed control eyes.

Despite differences in retinal thickness with SD-OCT, no obvious differences in retinal morphology were observed after blast exposure with either holder when using glutamine synthetase to probe for Muller glia and DAPI counterstaining to probe for nuclei in the outer nuclear layer (ONL), inner nuclear layer (INL), and ganglion cell layer (GCL) (Fig. 8A). Additionally, no evidence of cell death was observed in either blast-exposed group when using TUNEL staining to probe for apoptosis (Fig. 8B).

3.4 Rats showed cognitive deficits only with the open holder

Blast-exposed rats exhibited no differences in exploratory behavior (number of entries, Fig. 9A), regardless of holder. Blast-exposed rats immobilized using the open holder showed a 16% reduction in spatial alternation scores (spatial cognition) compared with control rats (Fig. 9B). Rats in the enclosed holder group exhibited significantly greater spatial alternation scores compared with rats in the open holder group (one-way ANOVA, F[2,28] = 3.841, $p < 0.05$, Fig. 9B); the former group's scores were statistically similar to those of controls.

3.5 Head movements differed during blast exposure between open and enclosed holders

In order to visualize the type of head movement occurring with each holder, live blast exposures were filmed at 3000 frames per second using a high-speed camera. The resultant

slow-motion videos showed that the rodents' heads do move from side to side with the open holder. However, the amount of movement was variable and may have depended on the size of the rodent and how much of their head and shoulders was protruding from the holder. With the enclosed holder, we were unable to fully visualize the rodent during the blast because the holders are opaque, but the rodents' heads did appear to move towards the contralateral holder wall and rebound off the wall with significant angular velocity, causing them to protrude through the window.

4. DISCUSSION

4.1 Animal holder configuration used in primary blast injury studies affected functional outcomes

Using a rat model of blast overpressure and two different holder configurations, we investigated the effects of the animal holding chamber on the magnitude of eye and brain injury. In the open holder, the body below the shoulders was encased, whereas the head was fully exposed and could move freely during blast exposure. With the enclosed holder, both the rat's head and body were encased, such that the blast reached the ipsilateral eye through a small window. Differential outcomes were observed, depending on the type of holder. Visual function, as measured by optomotor response, showed similar post-blast deficits in the ipsilateral eye; however, contralateral eyes showed more severe visual function deficits when using the enclosed vs. the open holder. Retinal function deficits, as measured by ERG, were not observed post-blast exposure using the open holder, either in amplitude or implicit time. Meanwhile, ERG a- and b-wave amplitudes were significantly reduced in both ipsilateral and contralateral blast-exposed eyes from rats immobilized using the enclosed holder. Retinal structure, as measured by SD-OCT, showed reduced total retinal thickness and external limiting membrane thickness in both ipsilateral and contralateral eyes exposed to blast using the enclosed, but not the open, holder. Cognitive deficits, as measured by Y-maze, were observed only when using the open holder, not with the enclosed holder.

Taken together, our results demonstrate that blast exposure likely caused similar damage to eyes ipsilateral to the blast front, regardless of holder configuration. With the open holder, the blast wave may be propagating through the head to cause partial damage to the contralateral eye. However, with the enclosed holder, the blast wave could be forcing the contralateral eye against the holder wall, causing a compressive or concussive injury. It is also possible that internal reflection of the blast wave off the wall of the enclosed holder causes secondary blast wave exposure to the contralateral eye. Using the open holder, head movement is relatively unrestrained; thus, the head and brain may experience whiplash (*coup-contracoup* injury).

4.2 Ipsilateral versus contralateral eye differences with blast exposure

4.2.1 Retinal and visual function—Other researchers have compared the effects of blast exposure on function of both ipsilateral and contralateral eyes (see Table 1 for specifics on species, blast exposure, timepoints, holder configurations, and outcomes). In a study by Mohan et al., pattern ERG was reported to decrease in both ipsilateral and contralateral blast-exposed eyes[37]. This pattern ERG deficit mirrors our flash ERG amplitude reduction

with the enclosed holder, although their study did not find flash ERG differences. Reiner et al. observed OMR deficits in both visual acuity and contrast sensitivity in both the ipsilateral and contralateral eyes[50]. This finding mirrors our OMR results with the enclosed holder, although their study found worse visual acuity deficits in the contralateral blast-exposed eye and worse contrast sensitivity deficits in the ipsilateral eye, while our study found similar deficits in both blast-exposed eyes with the enclosed holder. Rex and colleagues reported increased ERG amplitudes at 1 month post-blast for a- waves, b- waves, and oscillatory potentials (OP) 1 and 2 in ipsilateral eyes from wildtype (WT) mice, but no change in ERGs in contralateral eyes[32, 33, 36]. Similarly, much larger changes were reported in visual acuity in ipsilateral *vs.* contralateral eyes from WT mice[32, 36, 51]. In both eyes, the most dramatic changes in visual acuity were observed at 7 days post-blast and resolved over time. In research by DeMar et al., in which the blast was directed either face-on (both eyes, simultaneously) or to just one eye (uniocular), severe reductions in ERG amplitude were observed in the ipsilateral eye, but not the contralateral, eye in the uniocular blast-exposed group, but not the face-on blast-exposed group[30]. While the holder in that study appeared to be more similar to our open holder, the magnitude of the blast and the resulting histological and retinal function damage was much greater than in our study, making any comparisons difficult. Overall, our visual and retinal function findings are consistent with those previously reported. Any differences may be due to differences in the magnitude of the blast pressure, mode of delivery of the blast (*e.g.*, open field blast, *vs.* paint gun or shock tube, etc.), differences in the holders used to immobilize the animals during blast exposure, or differences in the animal species employed (rats *vs.* mice).

4.2.2 Retinal thickness changes with blast exposure—With SD-OCT, Reiner et al. observed retinal thinning in the INL and photoreceptor layers in the ipsilateral blast-exposed eyes, but thicker INL in the contralateral eyes[50]. Mohan et al. reported reduced retinal nerve fiber layer (RNFL) thickness in the ipsilateral, but not the contralateral, blast-exposed eyes, and interestingly, those results were only observed in young mice, not 8-month-old mice[37]. Bricker-Anthony et al. found both ipsilateral and contralateral blast-exposed eyes to have small retinal detachments at 7 days post-blast exposure[32, 36]. While the external limiting membrane and total retinal thinning we observed when using the enclosed holder is not identical to what others have found, the general trend seems to be one of retinal thinning as a consequence of blast exposure.

4.2.3 Factors affecting contralateral blast-exposed eyes—The visual function, retinal function, and retinal structure results presented above show that, in our work and work by others, the ipsilateral and contralateral blast-exposed eyes often exhibit different phenotypes. Histological results presented in the literature further support this idea of differential patterns of injury. Optic nerve axon loss and retinal GFAP increases at 30 days post-blast exposure were observed in ipsilateral blast-exposed eyes but not contralateral eyes in one study[52]. Meanwhile, in that same study, microglial activation was observed in ipsilateral eyes only at 3 days post-blast exposure, but in both ipsilateral and contralateral eyes at 30 days post-blast[52]. Bricker-Anthony et al. also found that the timing of cell death differed in ipsilateral *vs.* contralateral blast-exposed eyes, suggesting a different mechanism. Additionally, the optic nerves and olfactory epithelium – structures that would be damaged

by a blast wave propagating through the head – did not appear damaged[32, 36]. They suggested, and our work supports, that damage to the contralateral eye with blast exposure occurs due to concussive injury caused by the eye hitting the side of the animal holding chamber. Another possibility is that a rebound effect of the blast wave reflecting inside the holder is causing contralateral eye injury. Additionally, retinal changes in the contralateral eye could be due to direct connections from one eye to the other, a phenomenon that has been shown to occur in retinal morphology after unilateral optic nerve transection in rats[53] and in retinal physiology, which shows cross talk in intact conditions as well as well as changes in cross talk with unilateral intraocular elevation and injections of tetrodotoxin[54].

4.3 Cognitive deficits dependent on holder configuration with blast exposure

Here, we found that cognitive deficits, as measured by Y-maze, were observed with the open holder, in which the head could move relatively freely in response to the force of the blast, but not when using the enclosed holder. Similarly, in a compressed gas shock tube model, Goldstein et al. found significant cognitive deficits, as measured by Barnes maze performance, when the rodent's head was allowed to move about freely with blast exposure[22]. However, subsequent analysis of the rodent head movement in this model by another group suggests that the cognitive deficits may not be due to primary blast exposure, but instead secondarily to the impact of the mouse skull against the animal holder[55]. When the head was fixed in place, using nylon cable ties and a bite bar, cognitive deficits were not observed. Kinetic analysis showed that blast causes head oscillation at speeds that could damage the brain, while intracranial pressure recordings showed that the blast wave passed through the brain with minimal differences in pressure. Our results with the open holder suggest similar forces could be at work, *i.e.*, the blast wave pressure causes head acceleration that induces brain injury. Alternatively, with the open holder, a pillow was positioned against the contralateral side of the rat's head (see Figure 1F in Allen et al., 2018[40]), which could have created an impact point similar to the Ritzel study[55].

4.4 Clinical relevance, limitations, and future directions

The results presented here may have translational implications and potentially support the concepts that 1) both primary blast and concussive ocular injuries may present in patients who are exposed to a blast, and 2) rapid head acceleration due to blast overpressure causes brain injury. Hence, when evaluating blast-exposed patients, tertiary effects of blast exposure should be considered as well as the primary blast wave.

A number of factors can affect blast exposure, including the placement of the specimen (or animal), the distance of the specimen from the blast, the type of driver gas used (helium, nitrogen, etc.), the amount of pressure used, and whether the specimen is greater than 10% of the size of the blast tube opening. When specimens are larger than 10%, secondary reflection off the specimen changes the loading profile of the blast[56].

Additionally, this study clearly shows that it is important to consider head movement when designing animal holding chambers for experimentally modeling blast exposure. Open *vs.* enclosed holders may mimic different aspects that could be relevant to field conditions (*e.g.*, wearing *vs.* not wearing a helmet, or traveling on foot *vs.* in a vehicle). Helmets

have been studied in rodent models of concussive traumatic brain injury[57, 58] and auditory effects of blast exposure[59]. In concussion models, helmet use resulted in a milder, more diffuse axonal injury[58]. Interestingly, a change as small as 5 degrees in the angle of the rodent helmet could alter linear acceleration of the head by 8-31%[60]. In auditory models, rupture threshold for the tympanic membrane was lower in the shielded chinchillas (shield = a stainless steel cup placed over the head) than in the open field chinchillas due to the blast waveforms delivering greater energy at higher frequencies in the shielded animals[59]. Thus far, the effects of helmets on ocular injury post-blast exposure have not been studied in animal models. Studies by Nguyen and colleagues have simulated blast wave impact onto unprotected *vs.* goggle-protected eyes. Their findings suggest that the nose and brow serve to focus the blast wave onto the unprotected eye, whereas when wearing goggles, the blast wave is deflected away from the eye[61, 62]. Understanding how these different holders direct the blast wave may provide further insight into the cause of injury and the holder configuration-dependent differences that affect injury to the contralateral eye.

High speed videography to visualize head movement verified that the rodents' heads move from side to side with blast exposure when using the open holder, though, the amount of movement was variable. With the enclosed holder, the rodents' heads appeared to rebound off the contralateral holder wall with significant angular velocity.

This amount of angular movement was unexpected but is consistent with our findings of mild ERG deficits and retinal thinning with the enclosed holder but not the open holder. One limitation of our study was the inability to fully measure the dynamic movement of the head in each holder during blast exposure, and this presents an avenue for future investigation. Another limitation was that the ERG and SD-OCT data reported here do not match our earlier paper, in which we found supernormal ERGs and increased retinal thickness with blast exposure[40]. This difference may be due to differences in positioning the rats in the holder or due to the fact that we used littermate controls in this study but used age-matched non-littermate controls in our previous study.

An additional limitation is that the histology was only performed on tissue taken at 6-8 months post-blast. Thus, the lack of TUNEL-positive cells was not surprising. It would be interesting to probe markers such as TUNEL in eyes from rats euthanized at earlier timepoints, including in the acute phase after the initial insult (blast overpressure exposure).

Finally, it is interesting that, with the enclosed holder, ERG, SD-OCT, and OMR deficits were observed, while with the open holder, OMR deficits were observed in the absence of ERG and SD-OCT deficits. A potential explanation is that ERG and SD-OCT are specific measures of retinal function and structure, respectively. Meanwhile, OMR can reveal deficits anywhere along the visual-motor chain[43]. Blast exposure has been shown to result in diffuse axonal injury, concomitant with decreased axon function and molecular changes similar to advanced neurodegenerative disease. A limitation of this study is that pattern ERG recording, photopic and scotopic negative response measurement, and visual evoked potential recording were not assessed in blast-exposed animals. Future studies should utilize these and other methods as they investigate whether optic nerve and axonal damage are the cause of the reductions in optomotor response. This seems likely as the visual system has

the ability to alter the responsiveness of cortical neurons in response to decreasing electrical activity from the retina.

4.5 Conclusions

The type of animal holder configuration utilized in blast studies can significantly affect visual and cognitive outcomes. These results highlight the importance of considering other effects in addition to the primary blast wave when diagnosing visual changes after blast exposure in patients and when developing animal models of blast exposure.

Supplementary Material

Refer to Web version on PubMed Central for supplementary material.

Acknowledgments

We thank Rebecca Benz and Kristie Kilby (Buffalo VAMC VMU staff) for technical assistance in the course of this study.

Funding:

This work was supported by the Department of Veterans Affairs [Biomedical Laboratory Research & Development Merit Award (BX002439) to SJF & MTP and Research Career Scientist Award (15F-RCS-001 to SJF); Rehabilitation Research & Development Research Career Scientist Award (RX003134 to MTP) and Career Development Awards (RX002928 to RSA, RX002342 to AJF)], the Georgia Research Alliance (to CRE), and NEI Core Grant P30EY006360.

References

1. Wolf SJ, Bebarta VS, Bonnett CJ, Pons PT, Cantrill SV. Blast injuries. Lancet. 812009;374(9687):405–15. doi:10.1016/s0140-6736(09)60257-9 [PubMed: 19631372]
2. Hoge CW, McGurk D, Thomas JL, Cox AL, Engel CC, Castro CA. Mild traumatic brain injury in U.S. Soldiers returning from Iraq. N Engl J Med. 1312008;358(5):453–63. doi:10.1056/NEJMoa072972 [PubMed: 18234750]
3. Capó-Aponte JE, Urosevich TG, Temme LA, Tarbett AK, Sanghera NK. Visual dysfunctions and symptoms during the subacute stage of blast-induced mild traumatic brain injury. Mil Med. 72012;177(7):804–13. doi:10.7205/milmed-d-12-00061 [PubMed: 22808887]
4. Defense and Veterans Brain Injury Center. DoD worldwide numbers for TBI. Accessed November 15, 2020.
5. Chase RP, Nevin RL. Population estimates of undocumented incident traumatic brain injuries among combat-deployed US military personnel. J Head Trauma Rehabil. Jan-Feb2015;30(1):E57–64. doi:10.1097/htr.0000000000000061
6. Dougherty AL, MacGregor AJ, Han PP, Heltemes KJ, Galarneau MR. Visual dysfunction following blast-related traumatic brain injury from the battlefield. Brain Inj. 2011;25(1):8–13. doi:10.3109/02699052.2010.536195 [PubMed: 21117919]
7. Dutca LM, Stasheff SF, Hedberg-Buenz A, et al.Early detection of subclinical visual damage after blast-mediated TBI enables prevention of chronic visual deficit by treatment with P7C3-S243. Invest Ophthalmol Vis Sci. 1222014;55(12):8330–41. doi:10.1167/iovs.14-15468 [PubMed: 25468886]
8. Goodrich GL, Flyg HM, Kirby JE, Chang CY, Martinsen GL. Mechanisms of TBI and visual consequences in military and veteran populations. Optom Vis Sci. 22013;90(2):105–12. doi:10.1097/OPX.0b013e31827f15a1 [PubMed: 23314131]

9. Lemke S, Cockerham GC, Glynn-Milley C, Cockerham KP. Visual quality of life in veterans with blast-induced traumatic brain injury. JAMA Ophthalmol. 122013;131(12):1602–9. doi:10.1001/jamaophthalmol.2013.5028 [PubMed: 24136237]
10. Thach AB, Johnson AJ, Carroll RB, et al.Severe eye injuries in the war in Iraq, 2003-2005. Ophthalmology. 22008;115(2):377–82. doi:10.1016/j.ophtha.2007.04.032 [PubMed: 17904224]
11. Pieramici DJ, Sternberg P Jr., Aaberg TM Sr., et al.A system for classifying mechanical injuries of the eye (globe). The Ocular Trauma Classification Group. Am J Ophthalmol. 61997;123(6):820–31. doi:10.1016/s0002-9394(14)71132-8 [PubMed: 9535627]
12. Cockerham GC, Rice TA, Hewes EH, et al.Closed-eye ocular injuries in the Iraq and Afghanistan wars. N Engl J Med. 622011;364(22):2172–3. doi:10.1056/NEJMc1010683 [PubMed: 21631351]
13. Lemke S, Cockerham GC, Glynn-Milley C, Lin R, Cockerham KP. Automated Perimetry and Visual Dysfunction in Blast-Related Traumatic Brain Injury. Ophthalmology. 22016;123(2):415–424. doi:10.1016/j.ophtha.2015.10.003 [PubMed: 26581554]
14. Goodrich GL, Kirby J, Cockerham G, Ingalla SP, Lew HL. Visual function in patients of a polytrauma rehabilitation center: A descriptive study. J Rehabil Res Dev. 2007;44(7):929–36. doi:10.1682/jrrd.2007.01.0003 [PubMed: 18075950]
15. Coe CD, Bower KS, Brooks DB, Stutzman RD, Hammer JB. Effect of blast trauma and corneal foreign bodies on visual performance. Optom Vis Sci. 82010;87(8):604–11. doi:10.1097/OPX.0b013e3181e61bc0 [PubMed: 20512081]
16. Magone MT, Kwon E, Shin SY. Chronic visual dysfunction after blast-induced mild traumatic brain injury. J Rehabil Res Dev. 2014;51(1):71–80. doi:10.1682/jrrd.2013.01.0008 [PubMed: 24805895]
17. DeWalt GJ, Eldred WD. Visual system pathology in humans and animal models of blast injury. J Comp Neurol. 912017;525(13):2955–2967. doi:10.1002/cne.24252 [PubMed: 28560719]
18. Ling GS, Ecklund JM. Traumatic brain injury in modern war. Curr Opin Anaesthesiol. 42011;24(2):124–30. doi:10.1097/ACO.0b013e32834458da [PubMed: 21301332]
19. IOM (Institutes of Medicine). Pathophysiology of Blast Injury and Overview of Experimental Data. Gulf War and Health, volume 9: Long-term effects of blast exposures. Washington, DC: National Academies Press.; 2014:33–84:chap 3.
20. Morley MG, Nguyen JK, Heier JS, Shingleton BJ, Pasternak JF, Bower KS. Blast eye injuries: a review for first responders. Disaster Med Public Health Prep. 62010;4(2):154–60. doi:10.1001/dmp.v4n2.hra10003 [PubMed: 20526138]
21. McAllister TW. Neurobiological consequences of traumatic brain injury. Dialogues Clin Neurosci. 2011;13(3):287–300. [PubMed: 22033563]
22. Goldstein LE, Fisher AM, Tagge CA, et al.Chronic traumatic encephalopathy in blast-exposed military veterans and a blast neurotrauma mouse model. Sci Transl Med. 5162012;4(134):134ra60. doi:10.1126/scitranslmed.3003716
23. Gullotti DM, Beamer M, Panzer MB, et al.Significant head accelerations can influence immediate neurological impairments in a murine model of blast-induced traumatic brain injury. J Biomech Eng. 92014;136(9):091004. doi:10.1115/1.4027873 [PubMed: 24950710]
24. Courtney A, Courtney M. The Complexity of Biomechanics Causing Primary Blast-Induced Traumatic Brain Injury: A Review of Potential Mechanisms. Front Neurol. 2015;6:221. doi:10.3389/fneur.2015.00221 [PubMed: 26539158]
25. Donat CK, Yanez Lopez M, Sastre M, et al.From biomechanics to pathology: predicting axonal injury from patterns of strain after traumatic brain injury. Brain. 2122021;144(1):70–91. doi:10.1093/brain/awaa336 [PubMed: 33454735]
26. Cernak IAnimal models of head trauma. NeuroRx : the journal of the American Society for Experimental NeuroTherapeutics. 2005;2(3):410–422. doi:10.1602/neurorx.2.3.410 [PubMed: 16389305]
27. Hines-Beard J, Marchetta J, Gordon S, Chaum E, Geisert EE, Rex TS. A mouse model of ocular blast injury that induces closed globe anterior and posterior pole damage. Exp Eye Res. 62012;99:63–70. doi:10.1016/j.exer.2012.03.013 [PubMed: 22504073]
28. Kuehn R, Simard PF, Driscoll I, et al.Rodent model of direct cranial blast injury. J Neurotrauma. 102011;28(10):2155–69. doi:10.1089/neu.2010.1532 [PubMed: 21639724]

29. Zou YY, Kan EM, Lu J, et al.Primary blast injury-induced lesions in the retina of adult rats. J Neuroinflammation. 722013;10:79. doi:10.1186/1742-2094-10-79 [PubMed: 23819902]
30. DeMar J, Sharrow K, Hill M, Berman J, Oliver T, Long J. Effects of Primary Blast Overpressure on Retina and Optic Tract in Rats. Front Neurol. 2016;7:59. doi:10.3389/fneur.2016.00059 [PubMed: 27199884]
31. Petras JM, Bauman RA, Elsayed NM. Visual system degeneration induced by blast overpressure. Toxicology. 7251997;121(1):41–9. doi:10.1016/s0300-483x(97)03654-8 [PubMed: 9217314]
32. Bricker-Anthony C, Hines-Beard J, Rex TS. Molecular changes and vision loss in a mouse model of closed-globe blast trauma. Invest Ophthalmol Vis Sci. 732014;55(8):4853–62. doi:10.1167/iovs.14-14353 [PubMed: 24994864]
33. Bricker-Anthony C, Hines-Beard J, Rex TS. Eye-Directed Overpressure Airwave-Induced Trauma Causes Lasting Damage to the Anterior and Posterior Globe: A Model for Testing Cell-Based Therapies. J Ocul Pharmacol Ther. 62016;32(5):286–95. doi:10.1089/jop.2015.0104 [PubMed: 26982447]
34. Goldstein LE, McKee AC, Stanton PK. Considerations for animal models of blast-related traumatic brain injury and chronic traumatic encephalopathy. Alzheimers Res Ther. 2014;6(5):64. doi:10.1186/s13195-014-0064-3 [PubMed: 25478023]
35. Weichel ED, Colyer MH, Ludlow SE, Bower KS, Eiseman AS. Combat ocular trauma visual outcomes during operations iraqi and enduring freedom. Ophthalmology. 122008;115(12):2235–45. doi:10.1016/j.ophtha.2008.08.033 [PubMed: 19041478]
36. Bricker-Anthony C, Rex TS. Neurodegeneration and Vision Loss after Mild Blunt Trauma in the C57Bl/6 and DBA/2J Mouse. PLoS One. 2015;10(7):e0131921. doi:10.1371/journal.pone.0131921 [PubMed: 26148200]
37. Mohan K, Kecova H, Hernandez-Merino E, Kardon RH, Harper MM. Retinal ganglion cell damage in an experimental rodent model of blast-mediated traumatic brain injury. Invest Ophthalmol Vis Sci. 5152013;54(5):3440–50. doi:10.1167/iovs.12-11522 [PubMed: 23620426]
38. Koliatsos VE, Cernak I, Xu L, et al.A mouse model of blast injury to brain: initial pathological, neuropathological, and behavioral characterization. J Neuropathol Exp Neurol. 52011;70(5):399–416. doi:10.1097/NEN.0b013e3182189f06 [PubMed: 21487304]
39. Motulsky HJ, Brown RE. Detecting outliers when fitting data with nonlinear regression – a new method based on robust nonlinear regression and the false discovery rate. BMC Bioinformatics. 2006/3/09 2006;7(1):123. doi:10.1186/1471-2105-7-123 [PubMed: 16526949]
40. Allen RS, Motz CT, Feola A, et al.Long-Term Functional and Structural Consequences of Primary Blast Overpressure to the Eye. J Neurotrauma. 912018;35(17):2104–2116. doi:10.1089/neu.2017.5394 [PubMed: 29648979]
41. Turner PV, Albassam MA. Susceptibility of rats to corneal lesions after injectable anesthesia. Comp Med. 42005;55(2):175–82. [PubMed: 15884781]
42. Prusky GT, Alam NM, Beekman S, Douglas RM. Rapid quantification of adult and developing mouse spatial vision using a virtual optomotor system. Invest Ophthalmol Vis Sci. 122004;45(12):4611–6. doi:10.1167/iovs.04-0541 [PubMed: 15557474]
43. Douglas RM, Alam NM, Silver BD, McGill TJ, Tschetter WW, Prusky GT. Independent visual threshold measurements in the two eyes of freely moving rats and mice using a virtual-reality optokinetic system. Vis Neurosci. Sep-Oct2005;22(5):677–84. doi:10.1017/s0952523805225166 [PubMed: 16332278]
44. Gudapati K, Singh A, Clarkson-Townsend D, Feola AJ, Allen RS. Behavioral Assessment of Visual Function via Optomotor Response and Cognitive Function via Y-Maze in Diabetic Rats. J Vis Exp. 10232020;(164)doi:10.3791/61806
45. Prusky GT, Alam NM, Douglas RM. Enhancement of vision by monocular deprivation in adult mice. J Neurosci. 1182006;26(45):11554–61. doi:10.1523/jneurosci.3396-06.2006 [PubMed: 17093076]
46. Aung MH, Kim MK, Olson DE, Thule PM, Pardue MT. Early visual deficits in streptozotocin-induced diabetic long evans rats. Invest Ophthalmol Vis Sci. 2152013;54(2):1370–7. doi:10.1167/iovs.12-10927 [PubMed: 23372054]

47. Allen RS, Bales K, Feola A, Pardue MT. In vivo Structural Assessments of Ocular Disease in Rodent Models using Optical Coherence Tomography. J Vis Exp. 7242020; (161)doi:10.3791/61588
48. Maurice T, Bayle J, Privat A. Learning impairment following acute administration of the calcium channel antagonist nimodipine in mice. Behav Pharmacol. 31995;6(2):167–175. [PubMed: 11224324]
49. Tu C, Li J, Jiang X, et al.Ion-current-based proteomic profiling of the retina in a rat model of Smith-Lemli-Opitz syndrome. Mol Cell Proteomics. 122013;12(12):3583–98. doi:10.1074/mcp.M113.027847 [PubMed: 23979708]
50. Reiner A, Heldt SA, Presley CS, et al.Motor, visual and emotional deficits in mice after closed-head mild traumatic brain injury are alleviated by the novel CB2 inverse agonist SMM-189. Int J Mol Sci. 12312014;16(1):758–87. doi:10.3390/ijms16010758 [PubMed: 25561230]
51. Bricker-Anthony C, Hines-Beard J, D'Surney L, Rex TS. Erratum to: Exacerbation of blast-induced ocular trauma by an immune response. J Neuroinflammation. 2016:220. vol. 1.
52. Guley NM, Del Mar NA, Ragsdale T, et al.Amelioration of visual deficits and visual system pathology after mild TBI with the cannabinoid type-2 receptor inverse agonist SMM-189. Experimental eye research. 2019;182:109–124. doi:10.1016/j.exer.2019.03.013 [PubMed: 30922891]
53. Schremser JL, Williams TP. Photoreceptor plasticity in the albino rat retina following unilateral optic nerve section. Exp Eye Res. 91992;55(3):393–9. doi:10.1016/0014-4835(92)90111-5 [PubMed: 1426073]
54. Tang X, Tzekov R, Passaglia CL. Retinal cross talk in the mammalian visual system. J Neurophysiol. 612016;115(6):3018–29. doi:10.1152/jn.01137.2015 [PubMed: 26984426]
55. Needham CE, Ritzel D, Rule GT, Wiri S, Young L. Blast Testing Issues and TBI: Experimental Models That Lead to Wrong Conclusions. Front Neurol. 2015;6:72. doi:10.3389/fneur.2015.00072 [PubMed: 25904891]
56. Chandra N, Sundaramurthy A, Gupta RK. Validation of Laboratory Animal and Surrogate Human Models in Primary Blast Injury Studies. Mil Med. 32017;182(S1):105–113. doi:10.7205/milmed-d-16-00144 [PubMed: 28291460]
57. Ge X, Yu J, Huang S, et al.A novel repetitive mild traumatic brain injury mouse model for chronic traumatic encephalopathy research. J Neurosci Methods. 1012018;308:162–172. doi:10.1016/j.jneumeth.2018.07.021 [PubMed: 30076860]
58. Marmarou A, Foda MA, van den Brink W, Campbell J, Kita H, Demetriadou K. A new model of diffuse brain injury in rats. Part I: Pathophysiology and biomechanics. J Neurosurg. 21994;80(2):291–300. doi:10.3171/jns.1994.80.2.0291 [PubMed: 8283269]
59. Gan RZ, Nakmali D, Ji XD, Leckness K, Yokell Z. Mechanical damage of tympanic membrane in relation to impulse pressure waveform - A study in chinchillas. Hearing research. 2016;340:25–34. doi:10.1016/j.heares.2016.01.004 [PubMed: 26807796]
60. Zhou R, Li Y, Cavanaugh JM, Zhang L. Investigate the Variations of the Head and Brain Response in a Rodent Head Impact Acceleration Model by Finite Element Modeling. Front Bioeng Biotechnol. 2020;8:172. doi:10.3389/fbioe.2020.00172 [PubMed: 32258009]
61. Bailoor S, Bhardwaj R, Nguyen TD. Effectiveness of eye armor during blast loading. Biomech Model Mechanobiol. 112015;14(6):1227–37. doi:10.1007/s10237-015-0667-z [PubMed: 25828209]
62. Bhardwaj R, Ziegler K, Seo JH, Ramesh KT, Nguyen TD. A computational model of blast loading on the human eye. Biomech Model Mechanobiol. 12014;13(1):123–40. doi:10.1007/s10237-013-0490-3 [PubMed: 23591604]

Highlights

- Type of animal holder used in blast studies affects visual and cognitive outcomes
- Enclosed holders may cause secondary damage to the contralateral eye
- Damage may involve concussive injury or blast wave reflection off the holder wall
- Open holders may damage the brain due to head movement (whiplash)
- Effects other than the primary blast wave should be considered post-blast exposure

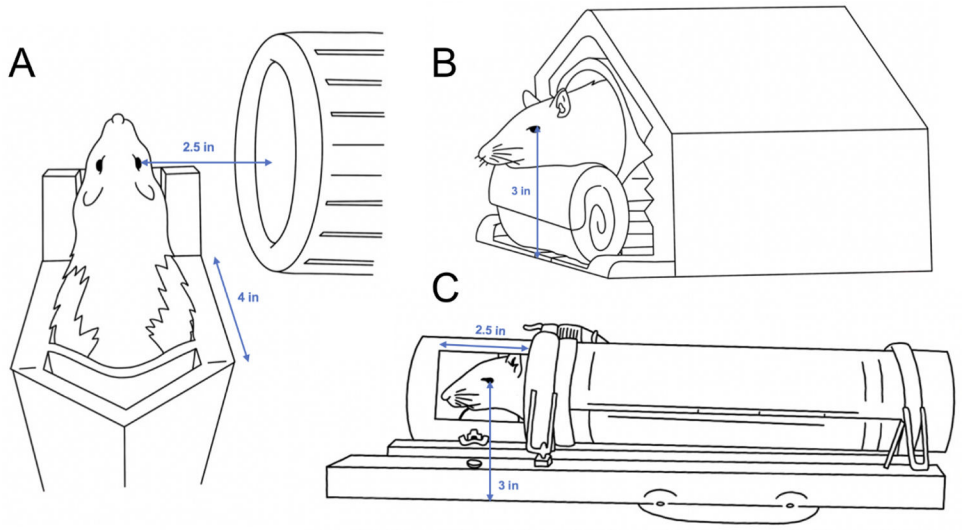

Figure 1. Animal holding chambers used during blast exposure.

The rats were positioned in open (A, B) or enclosed (C) holders during blast exposure. The blast wave passed the head of the rat perpendicular to the axis of the body, with one eye facing the blast wave (direct blast exposure), and with the contralateral eye shielded from direct blast exposure by the head of the rat. When using the open holder, a roll of gauze was placed under the rat's head as a support (B).

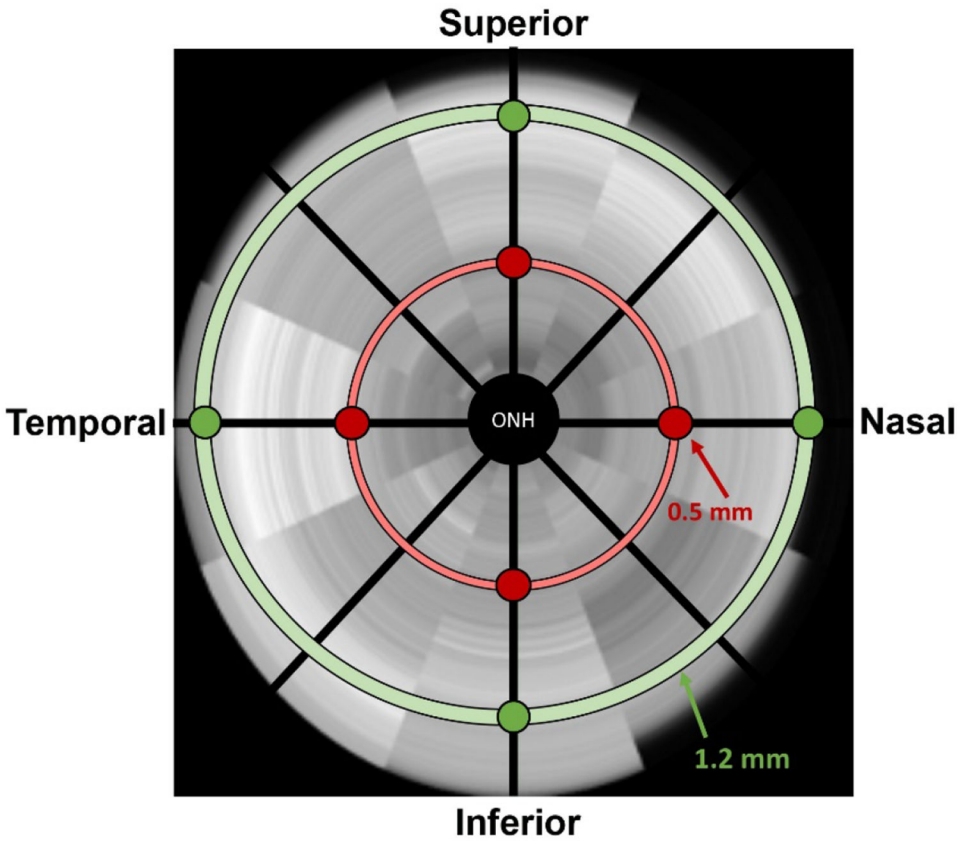

Figure 2. Diagram of OCT B-scan locations.

Images were captured at two distances from the optic nerve head, central (0.5 mm) and peripheral (1.2 mm), for four different quadrants or locations relative to the optic nerve.

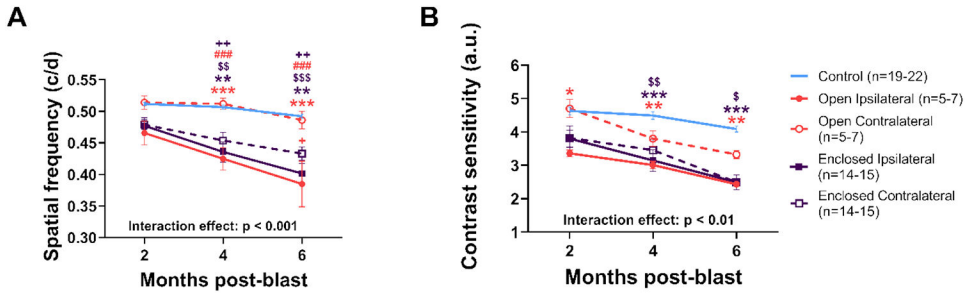

Figure 3: Visual function differentially affected in ipsilateral and contralateral blast-exposed eyes.

For both spatial frequency (A) and contrast sensitivity (B) thresholds, ipsilateral eyes from both holders and the contralateral eye from the enclosed holders were decreased while the contralateral eyes were completely spared from blast effects in rats from the open holder and partially spared with the enclosed holders. Colored symbols indicate comparisons with open (orange) or enclosed (purple) groups; * ipsilateral vs control eyes; $ contralateral vs control eyes; # ipsilateral vs contralateral; + ipsilateral to opposite holder contralateral. * $p < 0.05$, ** $p < 0.01$, *** $p < 0.001$, mean ± SEM.

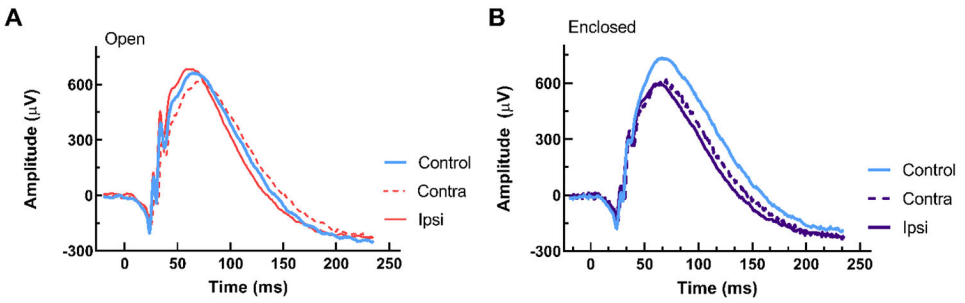

Figure 4. Representative ERG waveforms for open holder (A) and enclosed holder (B).

Representative dark-adapted ERG waveforms for control eyes (blue traces) versus ipsilateral (solid orange or purple traces) and contralateral blast-exposed eyes (dotted orange or purple traces) from rats at 6 months post-blast. Reduced a- and b- wave amplitudes were observed in blast and contralateral eyes with the enclosed holder (B).

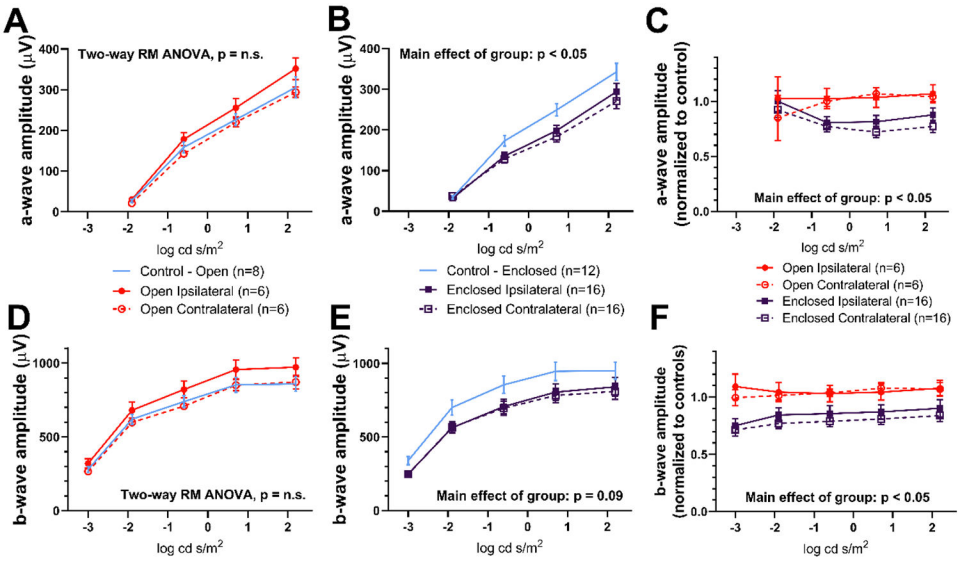

Figure 5. Reduced ERG amplitudes in enclosed holder rats.

ERG analysis for a- (A-C) and b- wave (D-F) amplitudes for rats exposed to blast in open (A, D) and enclosed holders (B, E). Amplitudes from rats in the open and enclosed holders were normalized (C, F). Eyes from the enclosed holder group showed smaller amplitudes than eyes from the open holder and control groups ($p < 0.05$), mean ± SEM.

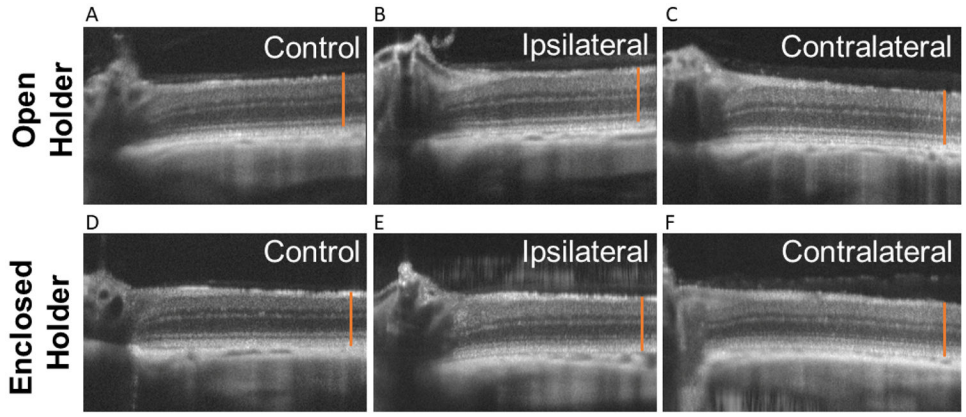

Figure 6. Representative spectral domain optical coherence tomography (SD-OCT) images for open holder (A-C) and enclosed holder (D-F).

Control eyes (A,D) versus ipsilateral (B,E) and contralateral blast-exposed eyes (C,F) from rats imaged at 6 months post-blast. The orange line is the same length for all images and extends from the retinal nerve fiber layer to the retinal pigmented epithelium in the control. Total retina and ELM thickness were reduced in both ipsilateral and contralateral eyes with the enclosed holder (E,F), compared to non-blast-exposed control eyes.

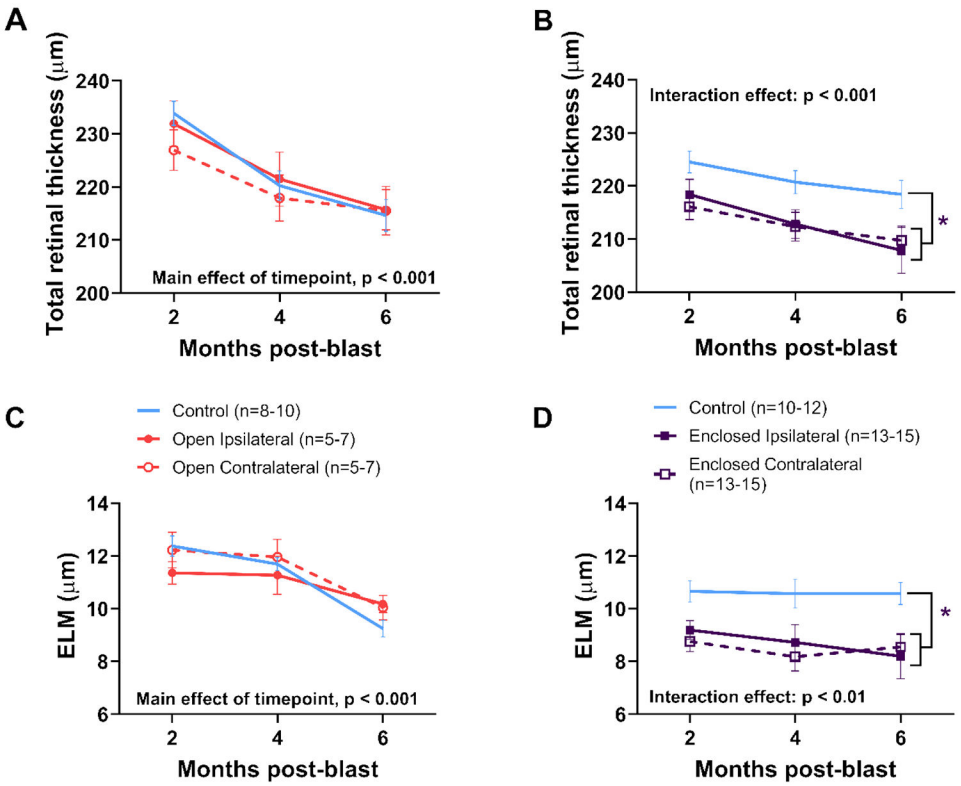

Figure 7. Thinner retinas in blast-exposed rats in enclosed holders.

SD-OCT analysis of total retinal (A-B) and external limiting membrane (ELM; C-D) thickness at 2, 4, and 6 months post-blast for rats in open (A, C) and enclosed holders (B, D) taken 0.5 mm from the optic nerve. The ipsilateral and contralateral blast-exposed eyes were significantly thinner, with respect to both total retinal (4%) and external limiting membrane (ELM) (18%) thickness, compared to non-blast-exposed control eyes. * $p < 0.05$, mean ± SEM.

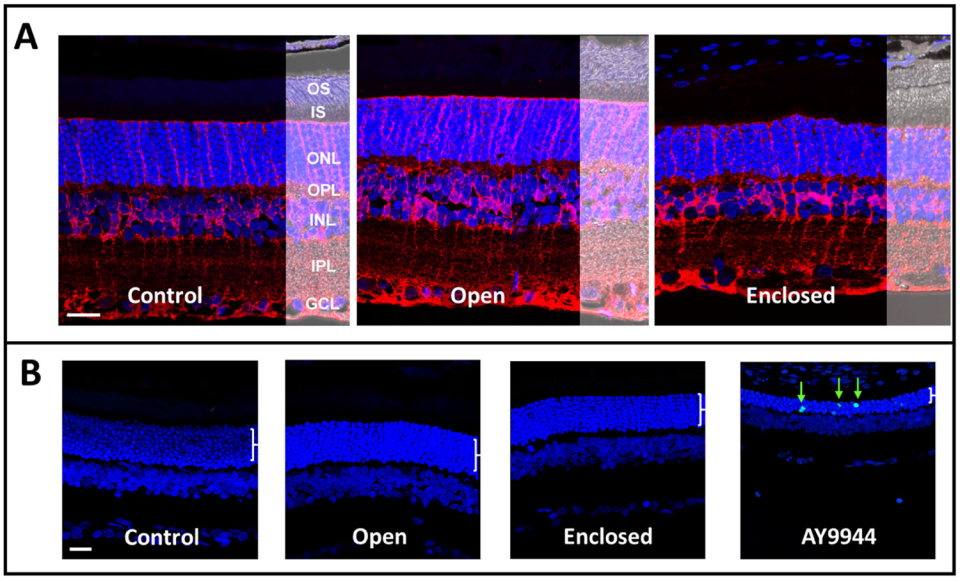

Figure 8. No obvious changes in retinal morphology or retinal cell death were observed in either blast-exposed group.

(**A**) Laser confocal immunofluorescence microscopy images of rat retinas (immersion PFA-fixed, paraffin embedded whole eyes) probed with antibody to glutamine synthetase (*red*) to label Muller glia processes, counterstained with DAPI (nuclei, *blue*), with Normarski image overlay to show retinal morphology. Control (non-blast exposed eyes) versus eyes from blast-exposed rats in open holder *vs.* enclosed holder, at 6-8 months post-blast exposure. No obvious differences in retinal morphology (*e.g.*, signs of degeneration) were observed as a function of blast exposure, relative to control. (**B**) Terminal deoxynucleotidyl transferase dUTP nick end labeling (TUNEL, *green arrows*) from each experimental group and eyes harvested from AY9944-treated rats serving as a biological positive control for apoptotic cell death. No overt signs of apoptosis in the ONL or other retinal layers at 6-8 months post-blast exposure. *Abbreviations*: OS, outer segment layer; IS, inner segment layer; ONL, outer nuclear layer; OPL, outer plexiform layer; INL, inner nuclear layer; IPL, inner plexiform layer; GCL, ganglion cell layer. Scale bar (all panels), 20 μM.

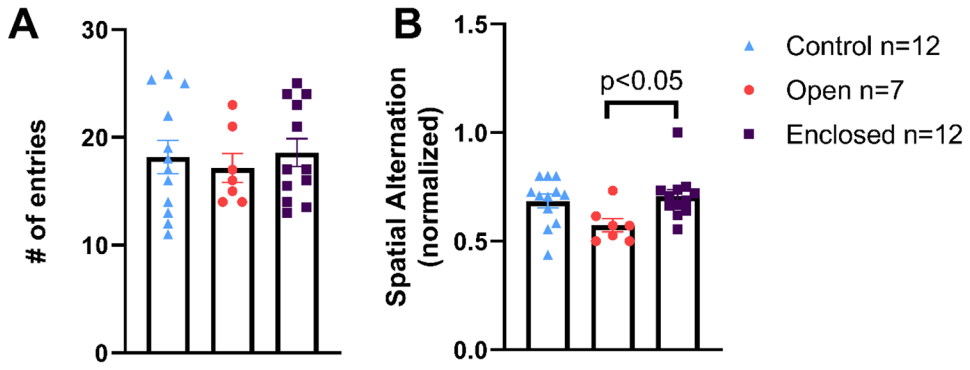

Figure 9. Spatial cognition deficits in rats exposed to blast in the open but not enclosed holder.

Exploratory behavior as measured by number of entries (A) and cognitive function (spatial cognition) as measured by spatial alternation (B) on Y-maze. Rats exposed to blast in the open holder experienced significant decrease in spatial cognition (B). * $p < 0.05$, mean ± SEM.

Table 1.

Literature review of the effects of blast exposure on function and structure of ipsilateral and contralateral eyes.

Reference	Species	Blast delivery	Holder	Timepoints	Major findings
Mohan et al., 2013	mouse	custom-built blast chamber 20psi	allowed head movement but more closely resembled our enclosed holder in schematics	1-24h, 7 days, 4-10 months	PERG: decreased amplitude in ipsilateral and contralateral ERG: no change (7 days) OCT: thinner RNFL in ipsilateral but not contralateral
Bricker-Anthony et al., 2014 and 2015	mouse	modified paintball gun 26psi	enclosed holder with very small window	3, 7, 14, 28 days	OMR: larger changes in visual acuity in ipsilateral vs. contralateral (resolved over time) ERG: increased amplitudes at 1 month in ipsilateral only OCT: small retinal detachments in both ipsilateral and contralateral Histology: timing of cell death different in ipsilateral vs contralateral
Reiner et al., 2015	mouse	modified paintball gun 50psi	enclosed with 7.5 mm opening between the eye and ear	2, 4 weeks (histology at 11 weeks)	OMR: decreased visual acuity and contrast sensitivity in ipsilateral and contralateral OCT: ipsilateral - thinning in INL and photoreceptor layers, contralateral - thicker INL
DeMar et al., 2016	rat	compression chamber attached to expansion chamber 20psi	nylon mesh sling attached to metal sled and inserted directly inside expansion chamber	1, 7, 14 days	ERG: severely reduced amplitudes in ipsilateral but not contralateral (in eye-blasted not face-blasted group)
Guley et al., 2019	mouse	modified paintball gun 50-60psi	enclosed with 7.5 mm opening between the eye and ear	3-7 days, 30 days	OMR: decreased contrast sensitivity in ipsilateral and contralateral Histology: Optic nerve loss and GFAP in ipsilateral only, microglial activation at 3 days in ipsilateral and at 30 days in both